DKIST Coronal Diagnostics

DKIST CSP Workshop #4

(G. Cauzzi for T. Schad)

Why ground-based optical/IR observations of the corona?

Following Landi, Habbal, & Tomczyk (2016) J. Geophys. Res. Space Physics, 121, 8237:

1. **CRITICAL(!) measurements of magnetic field through Hanle AND Zeeman effects.**
   X-ray and EUV lines do not provide this! B is small & Zeeman Effect prop. to. λ^2
2. **Single line temperature discriminants + multi-line thermal structure diagnostics**
   Comparable and complementary to EUV diagnostics.
3. **High spatial/spectral resolution instruments with extended field coverage.**
   The benefits of an EUV spectrometer combined with narrowband imaging (dynamics).
4. **Diagnostic potential out to several solar radii due to radiative excitation.**
   EUV diagnostics limited to <1.5 Rs. Note: DKIST pointing limited to <1.5 Rs.

The challenge of O/IR coronal spectral lines

- ***Very weak*** compared to solar disk continuum intensity ~(1-100) : 10^6 ----- > *limited to off-limb measurements*.
- Atmospheric and telescopic scattering of disk light challenging.
- Incomplete exploration and atomic data make IR lines a big discovery space. See recent del Zanna & DeLuca (2017) review.

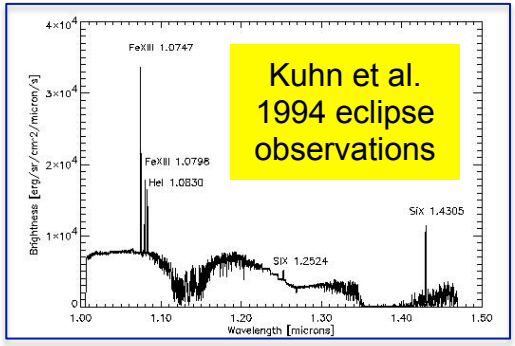

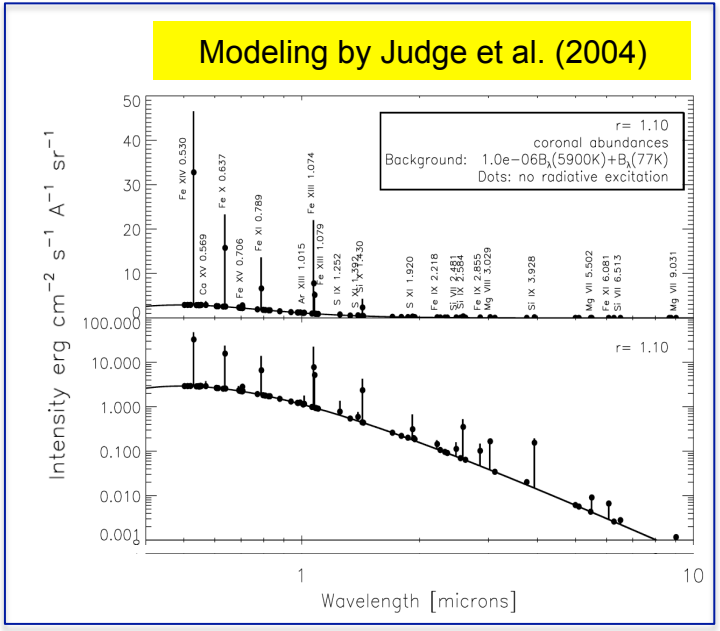

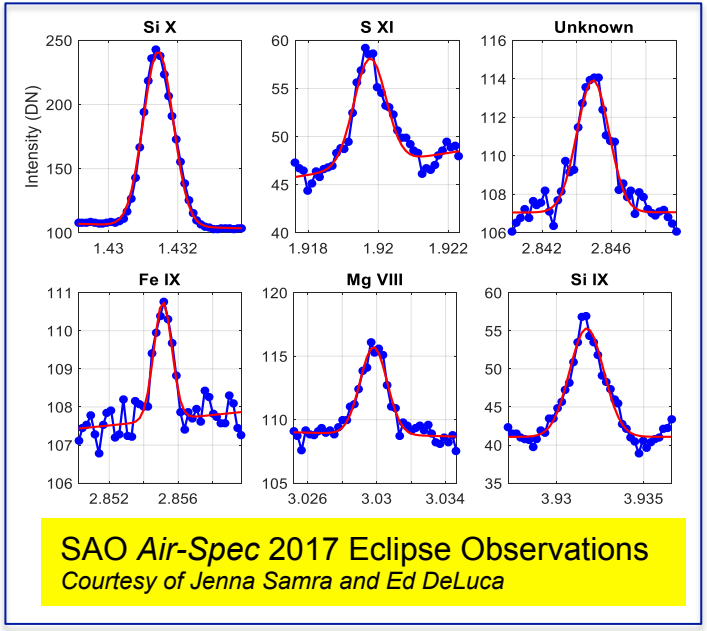

DKIST: Opening a new era in coronal diagnostics!

Revolutionary Coronal Features:

4 meter aperture → More photons!!
Access to the infrared:
- *All-reflective design (transmission out to 28 μm)*
- *First light instruments to 5 μm*

Minimizes scattered light by:
- *Off-axis design (no beam obscuration)*
- *High-grade M1 polish*
- *Cleaning procedures (CO_2 + washing)*
- *Access to the lower scatter infrared.*

Occulters and stops:
- *Inverse occulter at prime focus (large 5' FOV)*
- *Lyot stop at intermediary pupil*
- *Limb occulting at Gregorian focus*

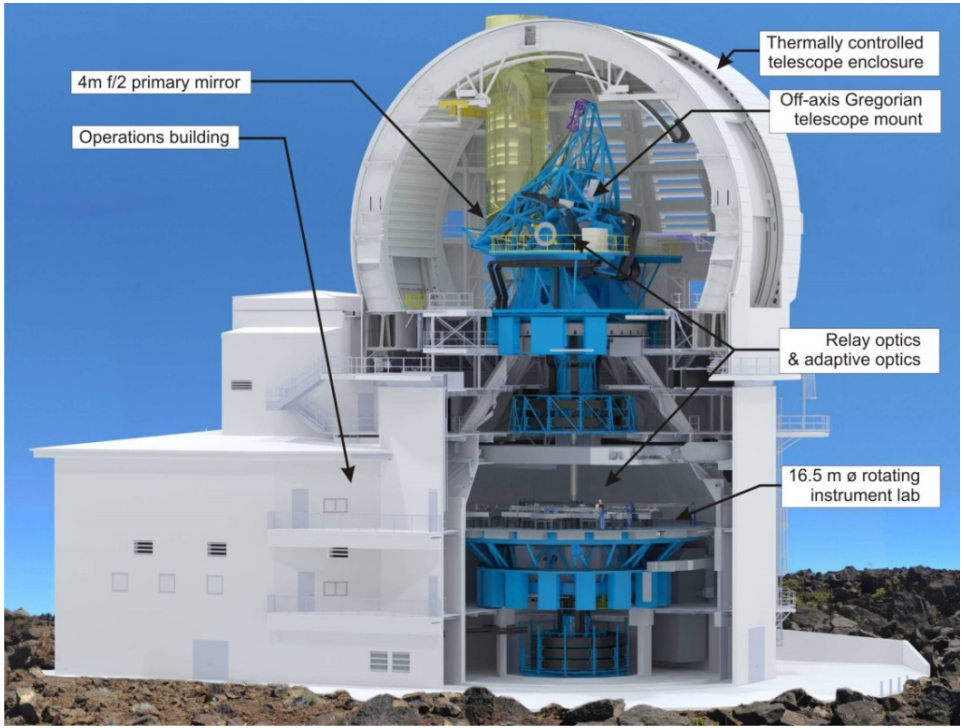

DKIST coronal diagnostics during early operations

- Emphasis on bright line observations with greatest magnetic field sensitivity.
- Corresponding peak temperature coverage: 1 to 1.6 MK
- Filter availability can be expanded in the future.

Maximum FOV: 2.8 arcmin -- Coordinated Operations

DL-NIRSP Spectropolarimetry

Fe XI λ7892 ; Log(T) ~ 6.13
Fe XIII λ10747 ; Log(T) ~ 6.22
Fe XIII λ10797 ; Log(T) ~ 6.22
He I λ10830 ; Log(T) ~ 4*
Si X λ14300 ; Log(T) ~ 6.13

VBI Imaging

Fe XI λ7892 ; Log(T) ~ 6.13

VISP Spectropolarimetry

Various lines: 380 to 900 nm
Including FeXIV 5303, FeX 6375,
(green + yellow lines)

Maximum FOV: 5 arcmin

Cryo-NIRSP Spectropolar.

Fe XIII λ10747 ; Log(T) ~ 6.22
Fe XIII λ10797 ; Log(T) ~ 6.22
He I λ10830 ; Log(T) ~ 4*
Si X λ14300 ; Log(T) ~ 6.13
Si IX λ39350 ; Log(T) ~ 6.04

Cryo-NIRSP Context Imager

Fe XIII λ10747 ; Log(T) ~ 6.22
He I λ10830 ; Log(T) ~ 4*
Si IX λ39340 ; Log(T) ~ 6.04

An introduction to DKIST coronal diagnostics

1. Polarized visible/IR line formation in the corona
2. Sensitivity estimates of background-limited measurements at DKIST
3. Techniques for extracting useful diagnostics

An introduction to DKIST coronal diagnostics

1. **Polarized visible/IR line formation in the corona**
2. Sensitivity estimates of background-limited measurements at DKIST
3. Techniques for extracting useful diagnostics

Line excitation mechanisms

- VIS/IR coronal spectral lines (unlike EUV lines) are both collisionally and radiatively excited. Using notation from Landi, Habbal, & Tomczyk (2016):

$$I_{\text{line}} = I_{\text{coll}} + I_{\text{rad}}$$

$$I_{\text{coll}} = \frac{1}{4\pi}\int_{-\infty}^{\infty} G(T, n_e)\varphi(T)\mathrm{d}T$$

$$I_{\text{rad}} = \frac{B}{4\pi}\frac{A_{ij}}{A_{\text{tot}}}\int_{-\infty}^{\infty} N_{abs}p(\phi)F_{inc}D(v)\mathrm{d}x$$

$$G_{ji}(T, n_e) = \frac{n_j(\mathrm{X}^{+q})}{n(\mathrm{X}^{+q})}\frac{n(\mathrm{X}^{+q})}{n(\mathrm{X})}\frac{n(\mathrm{X})}{n(\mathrm{H})}\frac{n(\mathrm{H})}{n_e}\frac{A_{ji}}{n_e}$$

Contribution function

$$\varphi(T) = n_e^2\frac{\mathrm{d}x}{\mathrm{d}T}$$

Differential Emission Measure (DEM)

$$N_{\text{abs}} = \frac{n(\mathrm{X}^{+q})}{n(\mathrm{X})}\frac{n(\mathrm{X})}{n(\mathrm{H})}\frac{n(\mathrm{H})}{n_e}n_e$$

Number of Absorbers

Incident radiation

- The contribution function, with corresponding level populations, can be calculated using CHIANTI, and is strongly peaked in temperature with a smaller dependence on source density.

Contribution functions for Cryo-NIRSP first light spectral lines

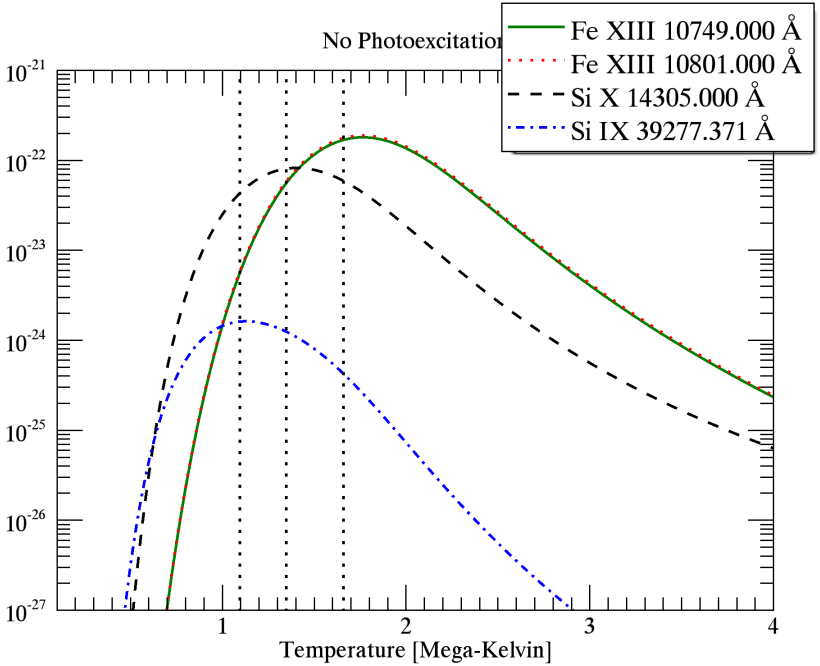

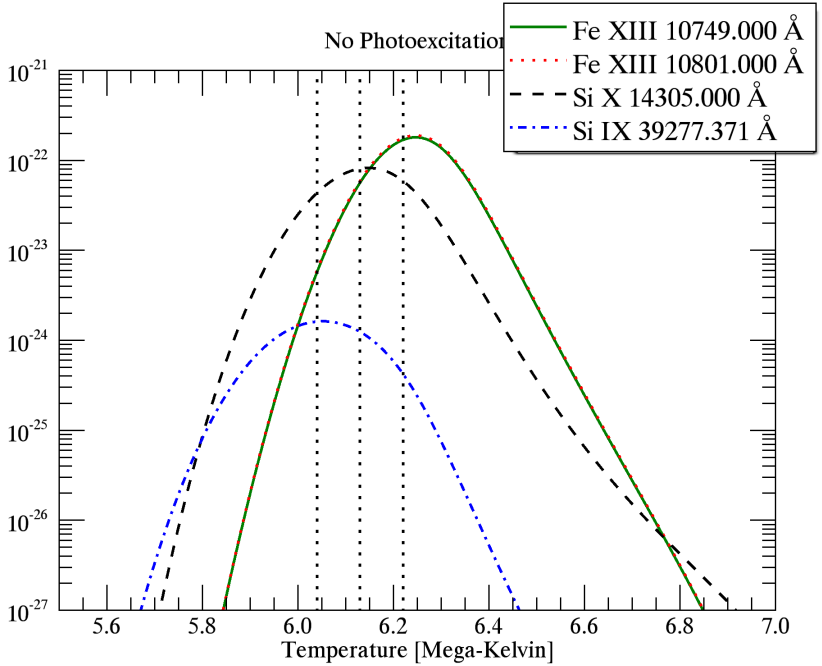

*Generated using CHIANTI v6 using default ionization equilibrium and coronal densities.

Consequences of the line excitation mechanisms

- I_{coll} strong function of n_e^2
  I_{rad} depends on n_e (similar to Thompson scattered K-continuum).
- *Extended morphological structures seen in white-light eclipse photos also expected in VIS/IR spectral intensity maps.*

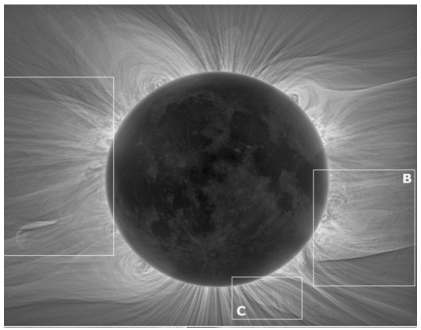

Druckmüller et al. 2014

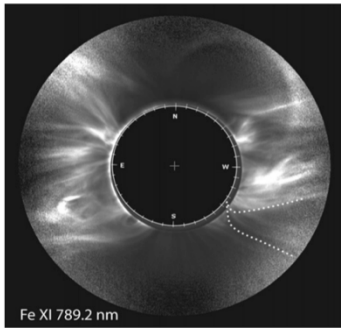

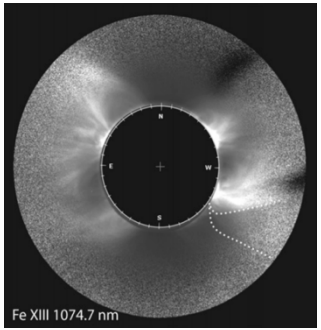

Habbal et al. 2011

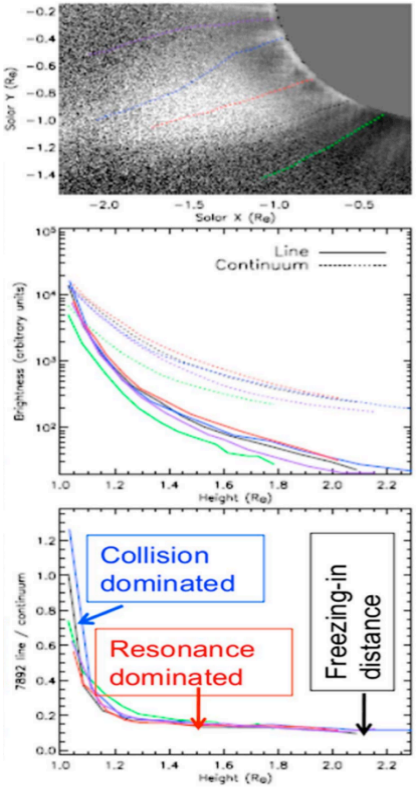

Habbal et al. 2007

- Analysis must include radiative correction unless collisionally dominated.
- Mechanisms can be diagnosed using line to (polarized-) continuum ratios. Also helpful to pair with EUV observations.

Formation of polarized signals in coronal lines

- VIS/IR coronal lines are typically magnetic-dipole (M1) transitions with polarization generated off-limb via:
  - *Anisotropic radiative excitation leads to optical pumping effect (i.e. scattering/atomic-level polarization)*
  - *The Zeeman Effect.*
- Atomic-level population balances/coherences are modified by both the ***Hanle Effect*** and ***Collisional Depolarization.***
- Long M1 radiative lifetimes means Hanle effect saturates (i.e. no field strength dependence) and collisions can be treated in CRD (complete redistribution -- no angular dependence).
- Zeeman splitting increases as $\lambda^2 \rightarrow$ *major driver of infrared coronal observations*!
  - *Low field strengths of corona make transverse Zeeman signals in Q,U too weak.*
  - *Stokes V signals typically 100x weaker than atomic level polarization.*

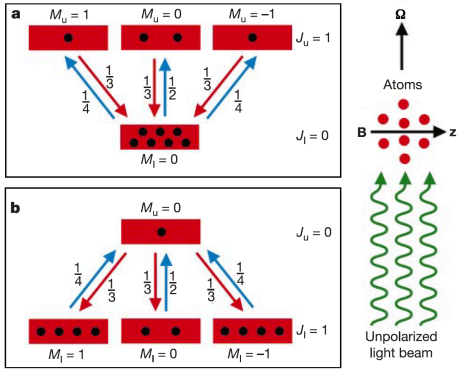

Upper- and lower-level population pumping
Trujillo Bueno (2002)

For a complete treatment of polarized formation see Casini & Judge (1999) ApJ, 522

Linear polarization is much easier to measure

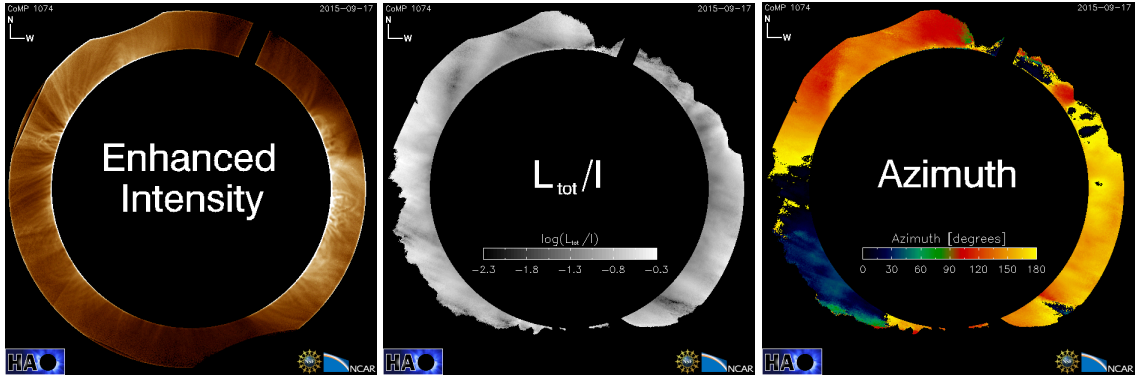

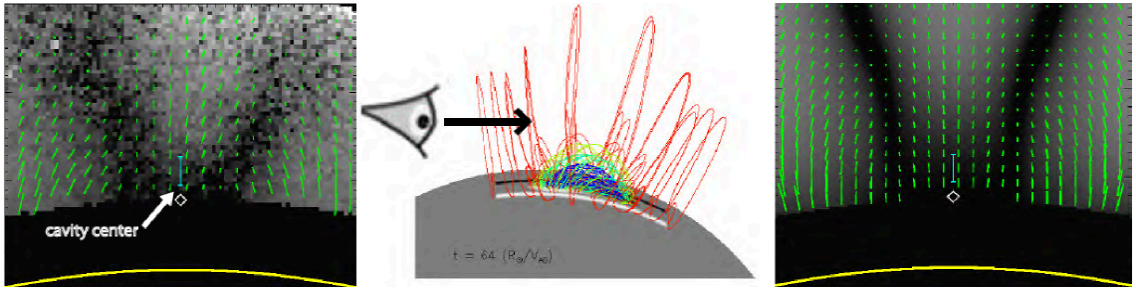

Linear polarization direction only sensitive to *magnetic azimuth in plane-of-sky*.

Amplitude depends on atomic orientation and requires detailed modeling to interpret.

Gibson (2017) and colleagues have shown linear polarization observations can discriminate models of coronal cavities.

Polarization nulls and directional change in polarization azimuth relate to Van Vleck ambiguities.

Measuring Stokes V is difficult and requires careful calibration

Fe XIII 1074.7 nm – Stokes Spectrum

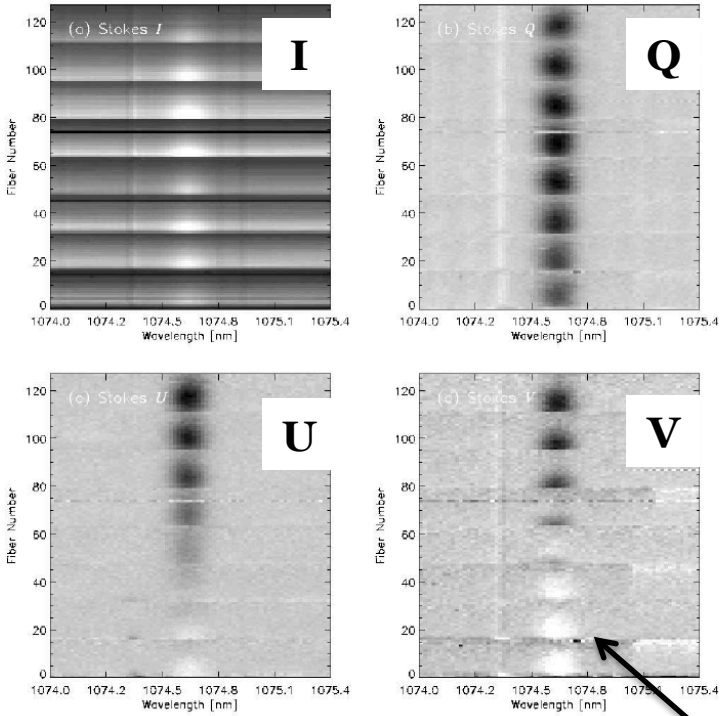

Lin, Kuhn, and Coulter (2004) recover Stokes V through least squares fitting of I+/- V measurements with crosstalk.

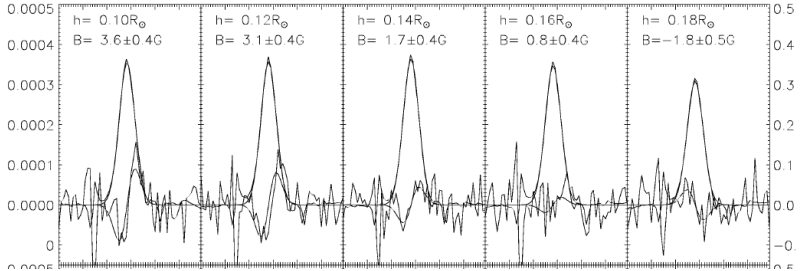

Circular polarization of spectral lines is sensitive to *longitudinal magnetic flux* (**B** cos Θ_B).

Amplitudes of circular polarization also depends on atomic alignment, which needs multiple lines to constrain or atomic polarization modeling.

Dominated by crosstalk

Relative detectability of coronal polarization

- Stokes V sensitivity: line brightness + λ^2 Zeeman Effect [*geff=1.5*] (Judge et al. 2001).
- Linear polarizability depends on atomic parameters, i.e. $W_2(J_l,J_u)$ from Landi Degl'Innocenti & Landolfi 2004 Table 10.1.
- Large differences in $W_2(J_l,J_u)$ may provide better multi-line constraints on atomic level polarization.

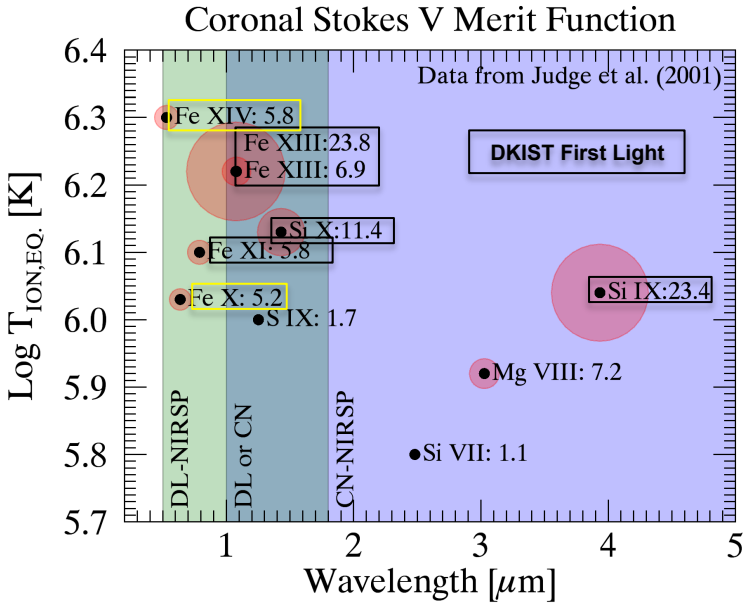

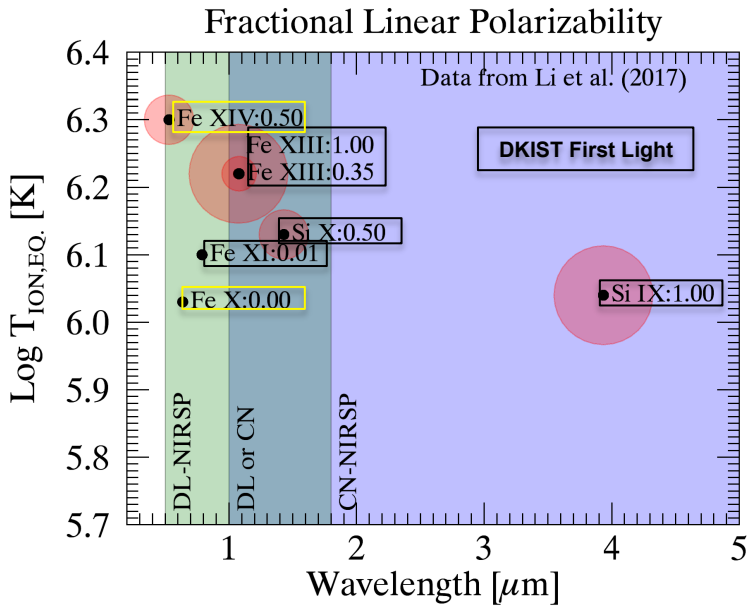

An introduction to DKIST coronal diagnostics

1. Polarized visible/IR line formation in the corona
2. **Sensitivity estimates of background-limited measurements at DKIST**
3. Techniques for extracting useful diagnostics

Background-limited measurements at DKIST.

$$\sigma = \sqrt{I_{tot}} = \sqrt{I_{Kcor} + I_{Fcor} + I_{Ecor} + I_{bg}}$$

- Emissive-corona (I_{Ecor}) of first-light lines typically > I_{kcor} > I_{Fcor}
  → Line intensities ≲ 10^{-5} of the disk intensity
  → QU & V polarization of a few-10% and ~ 10^{-4} of line signal, respectively.
  → *Circular polarization is ≲ 10^{-9} of disk intensity!*
- Background, $I_{bg,}$ originates from (1) scattering in the Earth's atmosphere, (2) telescope/instrument scattering, and (3) the thermal sky/instrument background.
- Haleakala coronal conditions excellent but variable.
- Telescope scattering due to microroughness and cleanliness of M1 with a requirement of 2.5 x 10^{-5} of the disk intensity at 1.1 solar radii and 1 micron *after washing*.
- Thermal background must be controlled by cryogenic cooling for Cryo-NIRSP.

Modeled contributions to coronal measurements

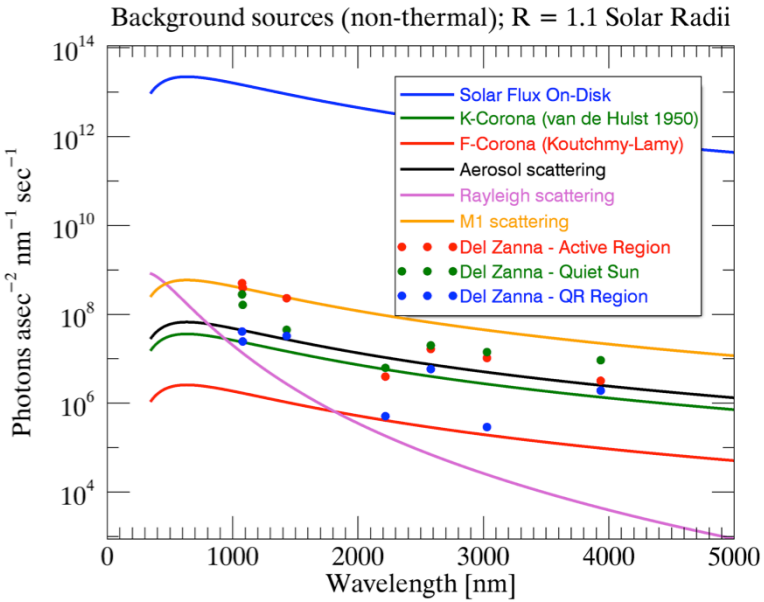

Thermal radiation background not included in this Figure.

- Modeled line radiances of ***select lines*** from Del Zanna & DeLuca (2017).
- Atmospheric scattering for excellent coronal skies.
- Primary mirror (M1) scattering *cleaned/washed* within 1 day of observation.
- *Occulters* at prime focus and gregorian focus limit illumination of downstream optics. *Lyot stop* rejects diffraction ring of primary.

The thermal background is non-negligible beyond ~2.5 microns

Cryo-NIRSP's spectrograph, cryogenically cooled, nearly eliminates out-of-band thermal flux.

In-band thermal background is a few factors below other radiative sources at the important 3.935 μm line.

Context imager has higher out-of-band thermal background.

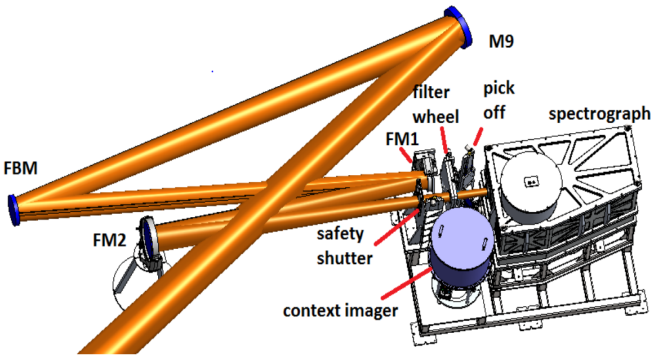

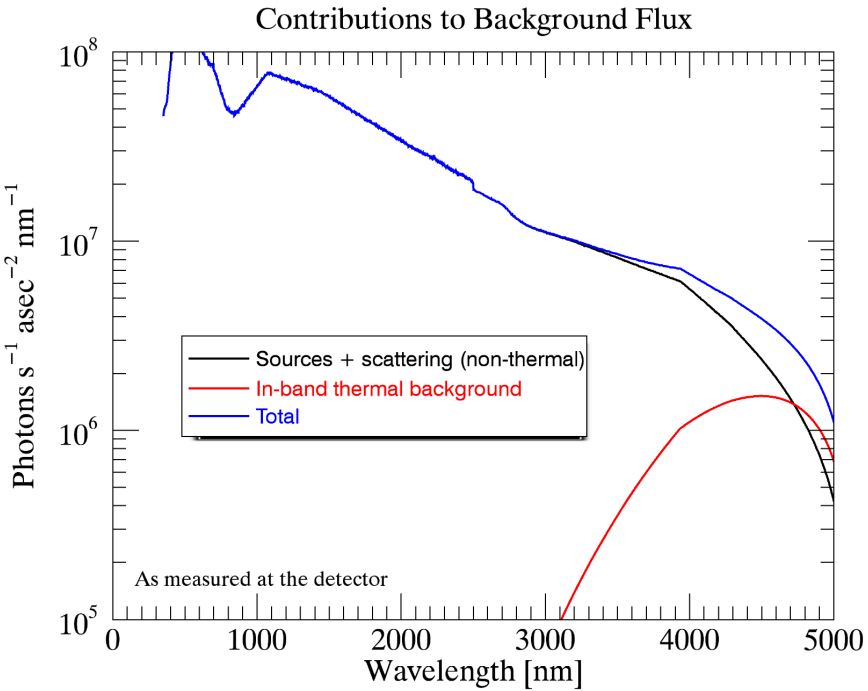

Monte-Carlo Determination of Measurement Sensitivities (Cryo-NIRSP)

Photon-noise only.

Long. Magnetic Field Error assumes weak-field approximation from single point.

Fe XIII and Si IX provides best B sensitivity.

See also Penn et al. (2004) for analytical error estimates.

Cryo-NIRSP Coronal Performance Estimates based on the QUIET REGION (QR) Model of Del Zanna & DeLuca (2017)
R = 1.1 solar radii
Background signals as specified in Figure 4 with read noise of 50 electrons per pixel.
Spatial integration assumes 0.5'' slit width and co-addition of 1'' along the slit.
Error values given for integration times of 1, 10, and 60 seconds as derived from a Monte Carlo simulation.
Errors represent photon noise only. Calibration limitations not included.

	Line radiance [photons cm^{-2} sec^{-1} $asec^{-2}$]	Inte-gration time [sec]	Integrated Intensity Error (dI/I) [percent]	Deg. of Linear Polarization Error [percent]	Line Width Error [percent]	Azimuthal Angle Error [degrees]	Doppler velocity error [m/sec]	Long. Mag. Field Error [Gauss]
Fe XIII 1074.7	240	1	0.09	0.19	0.13	1.05	11.8	10
		10	0.03	0.05	0.03	0.31	3.3	3
		60	0.01	0.02	0.01	0.12	1.3	2
Fe XIII 1079.7	140	1	0.16	0.31	0.21	1.79	19.7	16
		10	0.05	0.09	0.06	0.5	5.6	5
		60	0.02	0.03	0.02	0.2	2.2	2
Si X 1430	51	1	0.33	0.72	0.46	3.9	41.6	25
		10	0.09	0.19	0.13	1.07	11.7	7
		60	0.04	0.08	0.05	0.43	4.4	3
Fe IX 2218	11	1	1.13	3.81	1.59	59.53	146.9	57
		10	0.3	0.62	0.4	3.39	37.8	15
		60	0.12	0.24	0.16	1.34	15.2	6
Si IX 2580	41	1	0.32	0.7	0.46	3.85	41.8	14
		10	0.08	0.16	0.1	0.92	9.7	4
		60	0.03	0.06	0.04	0.37	4	2
Mg VIII 3028	34	1	0.42	1.19	0.56	15.32	51.4	14
		10	0.09	0.18	0.12	1.08	11.1	4
		60	0.04	0.07	0.05	0.42	4.5	2
Si IX 3935	29	1	0.38	0.74	0.5	4.2	47.6	11
		10	0.08	0.17	0.12	0.96	11.1	3
		60	0.03	0.07	0.04	0.38	4.6	1

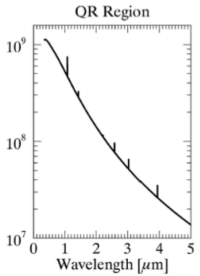

Coronal measurements with Cryo-NIRSP

Sit-and-stare observations and limited field-of-view rastering is available for temporal diagnostics of, e.g., oscillations.

Errors will be dependent on distance from solar limb.

4 x 3 arcmin Cryo-NIRSP scan ***with 1" step size will require between 1 and 3 hours for a magnetic field sensitivity of a few Gauss in a single wavelength.***

Must have a good understanding of what your use case demands.

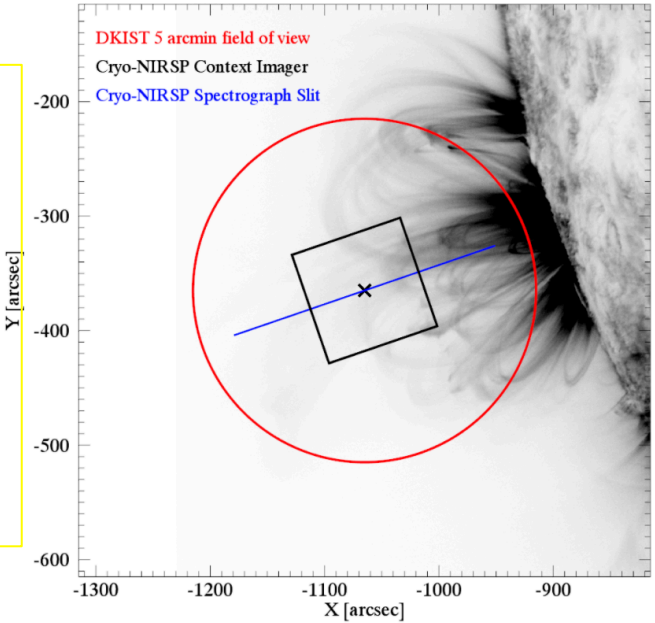

Coronal measurements with VISP, DL-NIRSP, and VBI

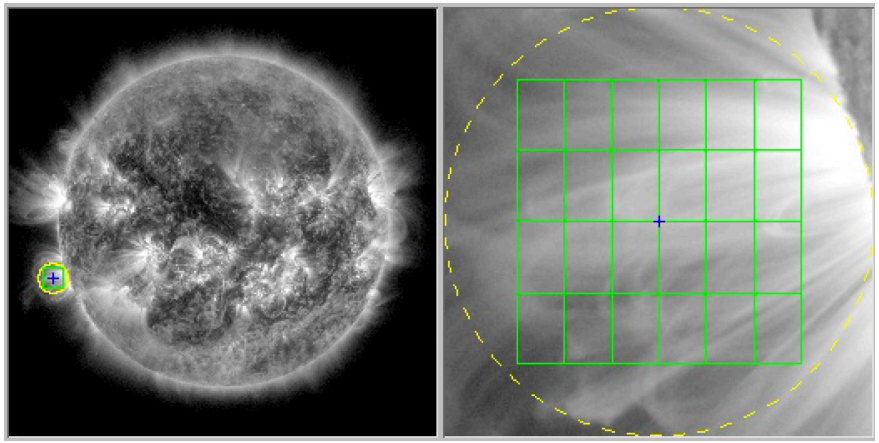

DL-NIRSP has a coarse sampling mode for coronal observations. 18'' x 28'' arcsec IFU coverage with multi-line coverage! Throughput less than CN.

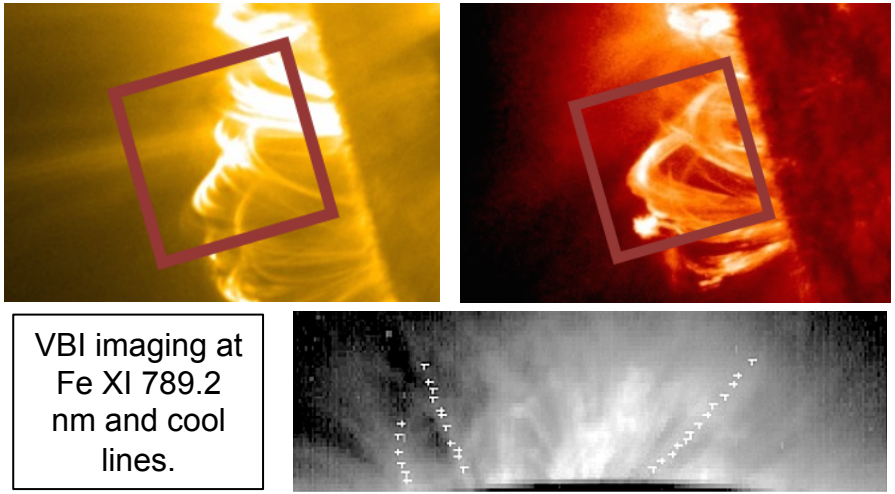

VBI imaging at Fe XI 789.2 nm and cool lines.

Singh, et al., 2006, *J. Astron Astr*, **27**, 115-124

+VISP rasters or sit-and-stare observations of visible coronal lines.

Understanding how to use DKIST coronal diagnostics

1. Polarized visible/IR line formation in the corona
2. Sensitivity estimates of background-limited measurements at DKIST
3. **Techniques for extracting useful diagnostics**

Techniques for extracting useful diagnostics – Part 1

Integrated quantities and radial dependencies:
[see Landi, Habbal, & Tomcyzk 2016; Del Zanna & DeLuca 2017]

a) **Electron density:** as function of radii distance can be related to continuum-polarized brightness
   i) DKIST Data → CN or DL full Stokes spectra with source separation.

b) **Plasma DEM, Φ(T):** constrained by VIS/IR lines using EUV analysis techniques when collisionally dominated and coordinated with EUV diagnostics.
   i) DKIST Data → VISP and DL, or CN intensity (or full Stokes) spectra.

c) **Elemental abundances** can be derived from line ratio of two charge states from same ion in radiatively dominated regime. Good for FIP analysis, for example of the solar wind source region.
   i) DKIST Data → Candidate first-light observation: Si IX 1430 nm and Si X 3935 nm. Future opportunities using only line pairs (see Del Zanna & DeLuca 2017).

d) **Electron density:** derived from line ratio of different transition of same ion with same charge state.
   i) DKIST Data → Sequential maps in Fe XIII line pair at 1074 nm and 1080 nm.

e) **Integrated longitudinal magnetic flux:** Stokes V observation in M1 line proportional to longitudinal magnetic flux.
   i) DKIST Data → CN or DL-NIRSP full Stokes spectra

f) **Non-thermal line broadening:** Turbulence diagnostic and/or discriminant for optically thin line-of-sight integration effects.
   i) DKIST Data → VISP and DL, or CN intensity (or full Stokes) spectra.

Techniques for extracting useful diagnostics – Part 2

Local structure morphology, dynamics, and single-point inversions
[see, e.g., Habbal et al. 2011; Judge, Habbal,& Landi 2013; Tomczyk et al. 2007]

a) **Temperature distribution/morphology**: Maps of spectral line intensity in different diagnostics provide thermal tomographic imaging.
  i) DKIST Data → CN or DL-NIRSP Stokes I spectral maps, CN context images, VBI 789.2 nm images.

b) **Doppler and translational velocities of eruptions**: Simultaneous imaging with spectral scans (or fast narrow FOV scans) give 3D velocity of eruptive events.
  i) DKIST Data → CN or DL-NIRSP Stokes I data cubes with CN or VBI imaging.

c) **Doppler shift oscillations and wave propagation**: Alfvenic/MHD wave propagation previously observed in VIS/IR lines; coronal seismology diagnostic).
  i) DKIST Data → CN slit or DL-NIRSP IFU Stokes I spectral data time series.

d) **Single-point inversion of coronal magnetic field:** Isolated structures identified in Stokes I maps suggest use of single-point magnetic field inversions [see Judge, Habbal,& Landi 2013 and Plowman 2014]
  i) DKIST Data → CN or DL-NIRSP Full Stokes mapped data cubes

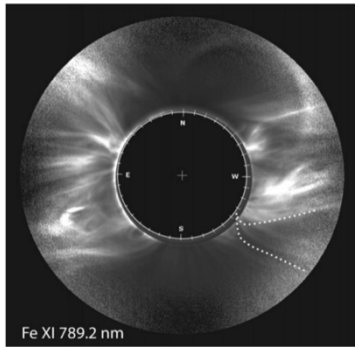

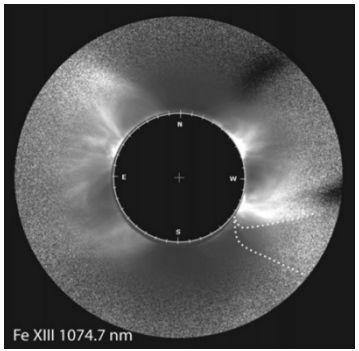

Habbal et al. 2011

Techniques for extracting useful diagnostics – Part 3

FORWARD *model comparisons using synthesized observables.*
[see, e.g., Gibson et al. Frontiers, 2016; Gibson et al. 2017; Dalmasse et al. 2016]

Data/model comparison of VIS/IR polarization diagnostics offer new constrains for numerical models of the 3D magnetic field including:

a) **Integrated linear polarization amplitude**
b) **Linear polarization direction in plane-of-sky**
c) **Integrated circular polarization amplitude**

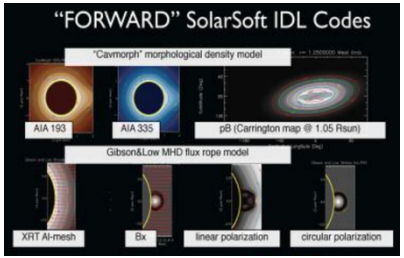

DKIST Data → CN or DL Full Stokes spectral data cubes in multiple spectral lines.

It's critical to include DKIST spectropolarimetric data as the primary magnetic model constraint within a range of coordinated EUV and VIS/IR observations.

Model-data fitting (i.e. inversions) techniques are in their infancy for coronal magnetometry. (see Dalmasse et al. 2016).

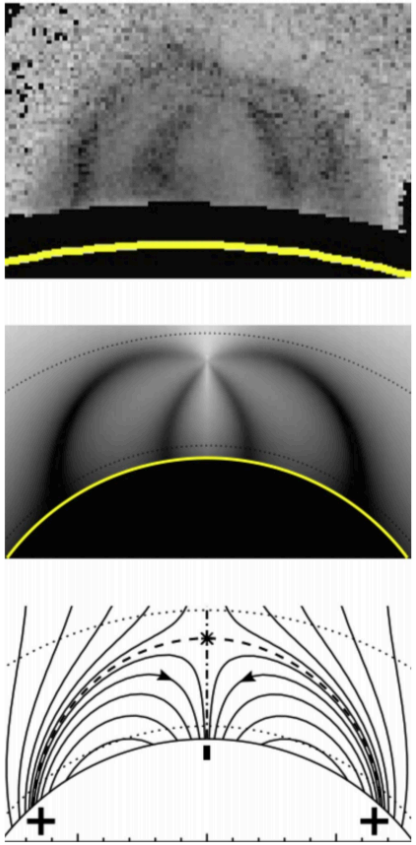

Gibson et al. 2017

Techniques for extracting useful diagnostics – Part 4

Tomographic inversions of coronal polarimetric data

[see, e.g., Kramer et al. , 2006, 2013, 2016.]

Multiple polarimetric observations of the same coronal volume along multiple line-of-sights can be used to perform tomographic inversions of the full 3D coronal magnetic field.

For stable regions, time separated tomography may have some applications using DKIST data. Using COMP data, this has been done by Kramar et al. 2016 for the global corona for one spectral line.

Kramar et al. 2016

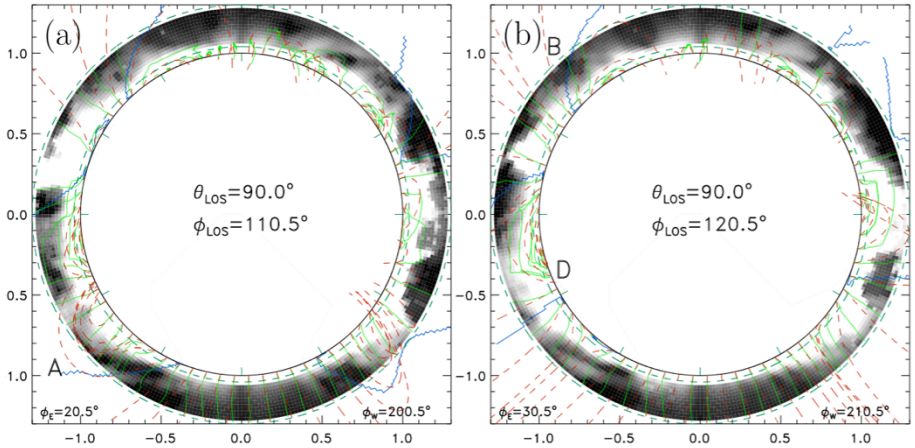

An introduction to DKIST coronal diagnostics - summarized

1. **Polarized visible/IR line formation in the corona**
   - Collisional and radiatively excited M1 transitions.
   - Polarization generated by the Zeeman Effect and resonance scattering in saturated regime.
   - DKIST first light spectral lines target high Stokes V sensitivity for magnetic field measurements.
2. **Sensitivity estimates of background-limited measurements at DKIST**
   - Coronal measurements from the ground are background-limited, which is variable.
   - Sensitivities based on models for background contributors and line radiances.
   - Cryo-NIRSP offers brand new capabilities for coronal spectroscopy of Si IX 3.9 um line.
3. **Techniques for extracting useful diagnostics**
   - Large range of diagnostics available.
   - Need community involvement to take full advantage of this new capability!

Looking forward to DKIST coronal science

- DKIST coronal diagnostics have broad applicability and provide critical capabilities to diagnose the coronal magnetic field.
- Both measurement and interpretation is challenging. We rely on the wealth of tools already available and those to come. For example, CHIANTI and FORWARD.
- Cryo-NIRSP IPC to be available later this spring. A CSP workshop dedicated to coronal science scheduled for June 2018.
- Community involved is critical to advance these diagnostics further.

Useful Resources on Optical/IR Coronal Diagnostics

References:

- Casini, R., White, S.M., Judge, P.G. (2017) *Magnetic Diagnostics of the Solar Corona: Synthesizing Optical and Radio Techniques*. Space Sci Rev,210, 145
- Del Zanna, G., & DeLuca, E. (2017) *Solar coronal lines in the visible and infrared. A rough guide.* ARXIV.
- Gibson, S. E., Rachmeler, L. A., White, S. M., eds. (2017). Coronal Magnetometry. Lausanne: Frontiers Media. doi: 10.3389/978-2-88945-220-0
- Judge, P.G., Habbal, S., Landi, E. (2013) *From Forbidden Coronal Lines to Meaninggul Coronal Magnetic Fields.* Solar Physics, 288, 267.
- Landi, E., Habbal, S.R., Tomczyk, S. (2016) *Coronal Plasma Diagnostics from Ground-Based Observations*. J. Geophys. Res. Space Physics, 121, 8237

Spectral line synthesis:

- Chianti v8 (http://www.chiantidatabase.org/)

Multiwavelength Coronal Forward Synthesis

- FORWARD (https://www2.hao.ucar.edu/modeling/FORWARD-home) [Gibson et al. 2016]